Hindawi Publishing Corporation
Journal of Nanomaterials
Volume 2015, Article ID 637124, 7 pages
http://dx.doi.org/10.1155/2015/637124

Research Article

Cathodo-, Thermo-, and Photoluminescent Properties of Nano-Y_2O_3:Eu^{3+} Fabricated by Controlled Combustion Synthesis

Tran Kim Anh,[1] Pham Thi Minh Chau,[1] Nguyen Thi Quy Hai,[1] and Le Quoc Minh[1,2]

[1]*Institute for Research and Development of High Technology, Duy Tan University, K7/25 Quang Trung, Hai Chau, Da Nang, Vietnam*
[2]*Vietnamese Academy of Science and Technology, 18 Hoang Quoc Viet, Cau Giay, Hanoi, Vietnam*

Correspondence should be addressed to Le Quoc Minh; lequocminhvn@gmail.com

Received 26 December 2014; Revised 19 March 2015; Accepted 20 March 2015

Academic Editor: Shifeng Zhou

Y_2O_3:Eu^{3+} nanophosphors were prepared through combustion reaction under controlled condition of the fuel ethylenediaminetetraacetic acid (EDTA-Na_2) and in the temperature range from 350 to 700°C. The products were characterized by X-ray diffraction (XRD), field emission scattering electron microscopy (FESEM), and energy dispersive spectroscopy (EDS). The results showed that Y_2O_3:Eu^{3+} nanoparticles were successfully synthesized by combustion method at low temperature and in short reaction time. The light-emitting ability of Y_2O_3:Eu^{3+} nanoparticles upon the electron excitation has been studied at the potentials 5, 10, and 15 kV. The thermoluminescent glow curves have elucidated an intense peak at 117°C after UV exposure and at least two peaks at 125 and 336°C with Gamma irradiation. Photoluminescent spectra of Y_2O_3:Eu^{3+} nanoparticles exhibited strong red luminescent color with highest sharp band at 612 nm under excitation in ultraviolet at 254, 394 and in visible at 465 nm. The dependence of photoluminescent properties of Y_2O_3:Eu^{3+} nanoparticles on annealing temperature and concentration of Eu^{3+} was also studied.

1. Introduction

Light emitting under electromagnetic fields exposure of the nanoparticles based on oxide yttrium (Y_2O_3) doped lanthanide (Ln) ions are become the promising way that open new opportunities for the application in various fields of electronics, optics and also biomedicine [1]. Yttrium oxide is a well-known host for transition metals and various lanthanide ions due to large band gap (5.8 eV), high dielectric constant, high thermal stability, and low cut-off phonon energy (380 cm^{-1}). The light emission efficiency of the nanomaterials based on Y_2O_3 doped with rare earth ions (Y_2O_3:Ln^{3+}) depends on the physical properties such as surface morphology [2], crystalline structures [3], and distribution of activator in matrix [4, 5]. High luminescence efficiency, long term thermal stability, high mechanical resistance, very good refractory properties, and chemical stability are interesting properties of Y_2O_3:Ln^{3+} [5]. Among them nano-Y_2O_3:Eu^{3+} has a great interest for application not only in the field emission display [6] and security printing [7] for electroluminescence [8], but also in biomedicine [9]. Nanoparticles synthesized by different methods show variation in their size, shape, and optical properties. To enhance the brightness and resolution of display of present technology, Y_2O_3:Ln^{3+} nanostructures of different morphologies have been synthesized by using sol-gel process [7, 10, 11], solvothermal [3, 12], hydrothermal [13, 14], colloidal and coprecipitation [15, 16], thermal and laser decomposition [17, 18], microwave [19], and combustion synthesis [7, 20–22]. Particularly, the combustion method has advantages due to its simplicity in nature and very short synthesis time. However, it is very important to develop phosphors nano-Y_2O_3:Eu^{3+} with controlled morphology and in particular the site-selectivity and relative behavior of the strongest $^5D_0$-$^7F_2$ (red) transition from Eu^{3+} needs to be further investigated for strong red phosphor application in the different fields.

In the present work Y_2O_3:Eu^{3+} nanoparticles were prepared by combustion method with EDTA-Na_2 and with urea for comparison. The structural and morphological properties were studied by using XRD, FESEM, and EDS. The cathodoluminescent (CL) and thermoluminescent (TL) properties of nano-Y_2O_3:Eu^{3+} have been investigated to explore

the application potential in display or dosimeter. The photoluminescent properties of the fabricated Y_2O_3:Eu^{3+} have been characterized by photoluminescence (PL) spectra and photoluminescence excitation (PLE) spectra to search for a novel red stronger luminescent nanophosphor based on Y_2O_3:Eu^{3+} to develop labeling or imaging tool in biomedicine.

2. Experiment

The sample was prepared by combustion method reported in [23]. All chemicals are of analytical grade. Yttrium oxide (99,99%, ALFA), europium oxide (99,95%, CERAC), nitric acid (99%, Sigma-Aldrich), EDTA-Na_2 (99%, Sigma), and urea (99.5%, Merck) were used as starting materials and fuels to prepare Y_2O_3:Eu^{3+}. Stoichiometric amounts of yttrium and europium oxides were dissolved in aqueous nitric acid 1 : 1 ratio. The solution was heated to 100°C on hot plate while being vigorously stirred until the solution became transparent. The reaction solution was dried at 70°C for 3 hours to remove the excess nitric acid and water. After cooling down to room temperature, the dried rare earth salts were mixed with small amount of EDTA-Na_2 in deionized water and vigorously stirred for 1 hour to form clear solution. Sealed containers with freshly prepared solution were then placed into an electrical oven heated up to 105°C for 1 hour. After that the containers were moved to Muffle furnace whose temperature was maintained at 350°C for 2 min and raised to 600°C for 3 min. The combustion process was completed in about 6–10 min. After completion of heating process the furnace cooled down to the room temperature. The fabricated compound was collected and washed with deionized water and ethanol and filtered to the ultimate white product, which was dried in vacuum at 70°C for 15 h to obtain Y_2O_3:Eu^{3+} fine powder. The obtained samples were foamy, fluffy, and porous.

The samples were checked by the X-ray diffractometer (XRD) Model Bruckner D8-Advance using Cu Kα, 40 kv, 20 mA. CL spectra, image, and EDS of Y_2O_3:Eu^{3+} were measured by field emission scattering electron microscope (FESEM) F 6400 JEOL. The PLE spectra and PL spectra of as-prepared and annealed samples were recorded using Spectrophotometer Model FL3-22 HORIBA with double monochromator, photomultiplier, appropriate lens and filters, and equipment NanoLog iHR 320 HORIBA Jobin Yvon. The samples preparation technique and measurement condition for luminescent intensities have been maintained throughout the entire experiment work. Therefore PL intensity results of the as-prepared or the annealing samples of Y_2O_3:Eu^{3+} could be compared precisely. The TL glow curves of Y_2O_3:Eu^{3+} were obtained in the temperature range of 50–450°C. The TL glow curves of Y_2O_3:Eu^{3+} were recorded with a homemade TL setup consisting of a small metallic plate heating strip, temperature programmer, photomultiplier tube, and multimeter recorder at heating rate of 2°Cs^{-1}. The TL glow curves obtained above were figured on using Origin software.

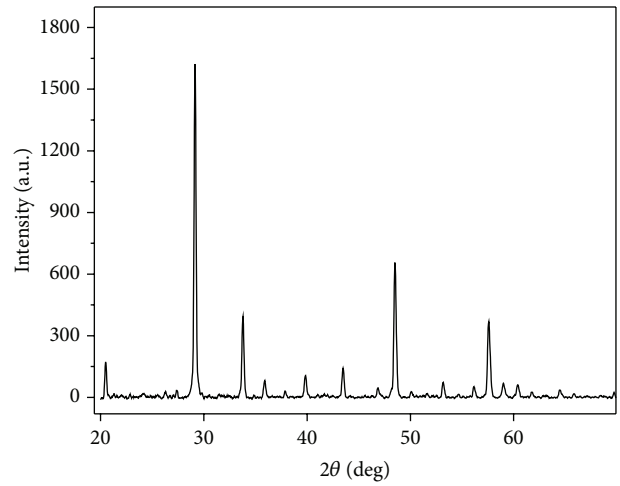

Figure 1: XRD spectra of Y_2O_3:5 mol% Eu^{3+}, annealed at 700°C.

3. Results and Discussion

The powder XRD patterns of Y_2O_3:5 mol% Eu^{3+} sample, which was prepared by combustion method with EDTA-Na_2 as fuel, annealed at 700°C, are shown in Figure 1. The appearance of all prominent diffraction peaks of the planes [222], [321], [411], [420], [332], [422], [440], and [145] corresponding to cubic form of yttrium oxide is in agreement with the JCPD41-1105. The particle sizes of these materials were estimated and found to be in the range of 24 nm for ~350°C and 26 nm for 700°C annealed sample. The obtained data were calculated by using the Scherrer equation [23].

These calculated particles sizes were in good agreement with those from FESEM images shown in Figure 2. This indicates the spatial structure, fluffy nature with pores, and voids with loosely agglomerated particles. The morphology of the synthesized samples depends on the nature and concentration of EDTA-Na_2 or urea as organic fuel. During combustion, yttrium nitrate impregnates into the amorphous product and gets ignited. Heat dissipates by the evolution of gaseous products in minimization and thus it leads to localization of heat due to amorphous nature of the fuel. Further increasing to about 800°C for 2 hours did not much affect the morphology with particles still having a large degree of porosity and agglomeration [24].

These estimated particles sizes of Y_2O_3:5 mol% Eu^{3+} prepared by combustion reaction in using EDTA-Na_2 as fuel were greater than those of Y_2O_3:5 mol% Eu^{3+} synthesized with urea $CO(NH_2)_2$ [7]. During the reaction process the reaction mixture underwent thermal dehydration and ignited at one spot with liberation of gaseous products such as oxides of nitrogen and carbon. The gaseous products during combustion reaction were liberated which increased surface area of powder products [25]. For the reaction mixture of EDTA-Na_2 need without further of any external heating. The heat of reaction is sufficient for decomposition of the mixture and resulted in the formation of particles. The combustion with urea can be controlled rate of the decomposition that

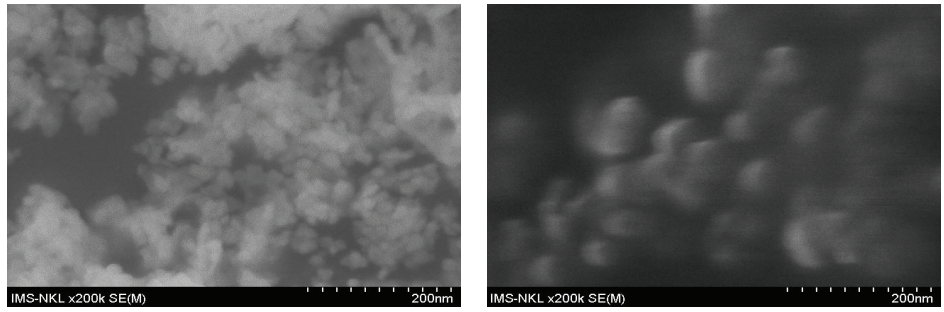

(a) (b)

Figure 2: (a) FESEM image of Y_2O_3:5 mol% Eu^{3+} annealed at 350°C. (b) FESEM image of Y_2O_3:5 mol% Eu^{3+} annealed at 700°C.

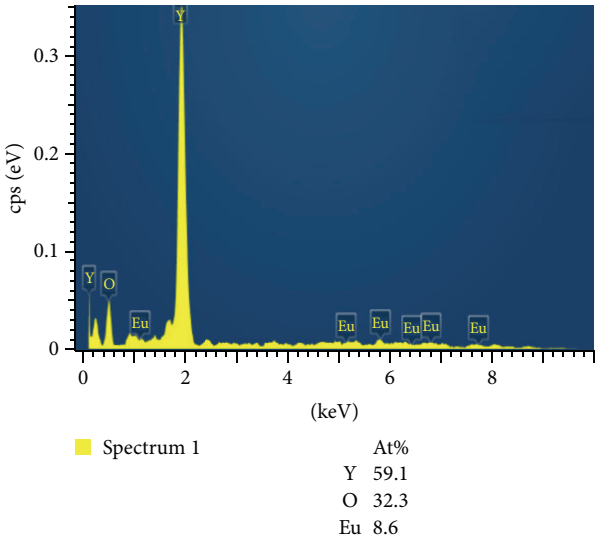

Figure 3: EDS of Y_2O_3:3% mol Eu^{3+}.

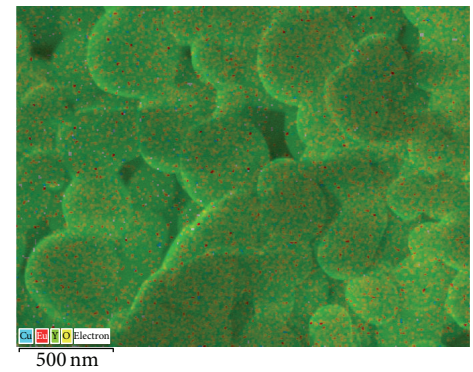

Figure 4: EDS layered image of Y_2O_3:Eu^{3+}.

would result in formation of particles with a small size and uniform distribution [23].

Figure 3 shows EDS spectrum of Y_2O_3:3 mol% Eu^{3+} sample, which shows that the product consists of the elements Y, O, and Eu. The EDS result in Figure 2 confirms the fabricated products were Y_2O_3 doped with Eu^{3+} ions. Figure 4 presents EDS layered image of Y_2O_3:3 mol% Eu^{3+} sample, in which the position of ions yttrium (green), oxygen (yellow), and europium (red dot) on yttrium oxide nanoparticles Y_2O_3 can be recognized. Based on these EDS spectra it can be considered that Eu^{3+} ions were distributed rather regularly on the particles of yttrium oxide doped europium ions.

3.1. Cathodoluminescence. Nanophosphors are efficient luminescent materials and irreplaceable components of light-emitting devices like cathode ray tubes, plasma display panels, and field emission display [26]. The last ones have been recognized as one of the most promising technologies due to their most important features like great brightness, wide horizontal and vertical view angels, good contrast ration, and wide work temperature range. One of the most promising solutions is lanthanide doped oxides, garnets, and some perovskites [27–29]. Therefore we have studied the light-emitting ability of Y_2O_3:Eu^{3+} nanoparticles upon the electron excitation. CL spectra were measured by F 6400 JEOL system, which were observed upon the different potentials of 5, 10, and 15 kV in high vacuum of 10^{-7} mmHg. In Figure 5 are presented the CL spectra of Y_2O_3:3 mol% Eu^{3+} samples and it is indicated that our samples have strong CL intensity even at low doping concentration of 3 mol% Eu^{3+}. These results have indicated that the obtained Y_2O_3:Eu^{3+} can be applied for display technology.

3.2. Thermoluminescence. Recent studies on different luminescent nanomaterials have shown a potential application in dosimeter of ionizing radiation for measurements of high doses using the TL technique [21, 30]. RE^{3+} doped Y_2O_3 material is one of such promising materials and some attention has been paid to study its TL characteristics. In 1996 Yeh and Su have reported the possible use of rare earth doped oxide phosphor in UV light dosimeter and found that Y_2O_3:Eu^{3+} is sensitive enough to measure background UV radiation such as sun light and bulb light [31]. Therefore they have investigated the TL behavior of Y_2O_3:Eu^{3+} after UV exposure. In this report the primary results of TL glow curves of Y_2O_3:5 mol% Eu^{3+} after UV exposure and Gamma irradiation are presented for comparison.

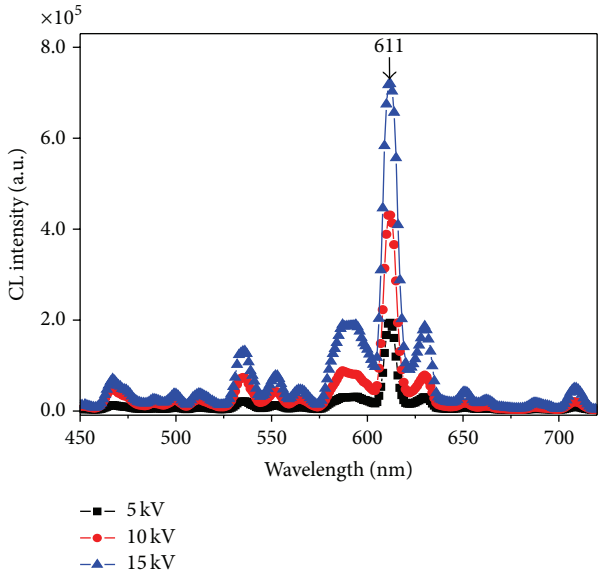

FIGURE 5: CL spectra of Y_2O_3:3 mol% Eu^{3+}. Black curve: 5 kV, red curve: 10 kV, and blue curve: 15 kV.

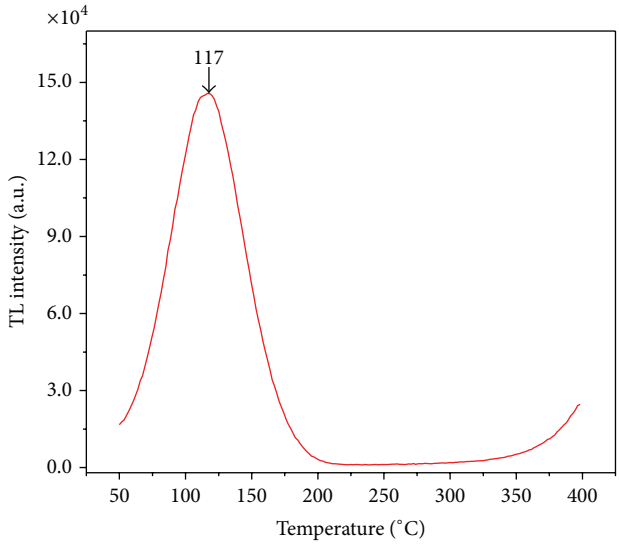

FIGURE 6: TL glow curve upon UV exposing.

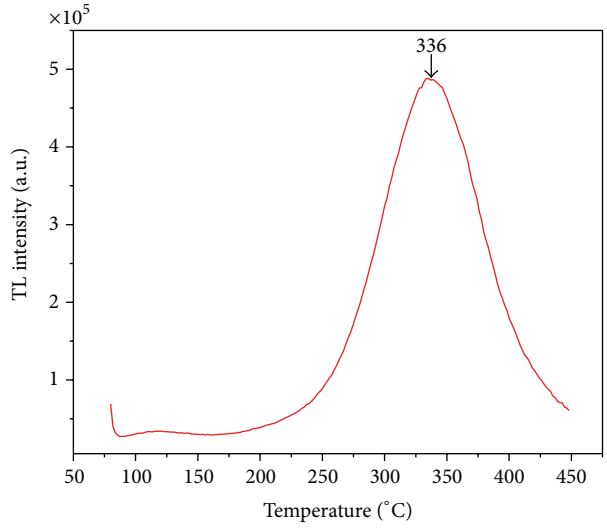

FIGURE 7: TL glow curve upon Gamma irradiation.

The Y_2O_3:Eu^{3+} samples were irradiated with D2 Lampe for 1 min and with a Gamma source for 75 h, and then their TL glow curves were recorded. The TL glow curve of Y_2O_3:5 mol% Eu^{3+} after UV irradiation was measured from 50°C to 400°C with the heating rate 2°C/sec. These TL glow curves were figured on using Origin software and one intense peak that appeared at 117°C was well resolved as can be seen in Figure 6. In the case of Gamma ray irradiation, the TL glow curves of Y_2O_3:Eu^{3+} sample for a dose of 9 mSv and exposure time 75 h, at least one prominent TL glow peak at 336°C was found (Figure 7). Tamrakar indicated that the TL glow curve of UV irradiated sample RE doped nanophosphor shows the formation of shallow trap (surface trapping) and the Gamma irradiated sample shows the formation of deep trapping [32, 33]. The estimation of trap formation was evaluated by knowledge of trapping parameters. The trapping parameters such as activation energy, order of kinetics, and frequency factor were calculated by peak shape method. Here most of the peak shows second order of kinetics. It is possible in UV irradiated Y_2O_3:Eu^{3+} phosphors that the TL response mainly generates from the traps on surface. Since these radiations cannot penetrate deeper and hence will not induce lattice defects may be caused by the trapped carriers which are produced during the sample processing.

3.3. Photoluminescence. In order to study the influence of excitation energy, the sample Y_2O_3 doped with 3 mol%, 5 mol% Eu^{3+} synthesized in using EDTA-Na_2 was excited by different wavelengths of 254, 465, and 394 nm from HORIBA system. All the samples showed strong PL emission with peak maximum at 612 nm under an excitation wavelength of 254 nm (Figure 8). We can note that the emission intensity when excited by the 254 nm wavelength was 1.6 times stronger than excitation by 394 nm. The spectra structure showed characteristic optical properties of Eu^{3+} ions in the cubic Y_2O_3 host [21]. The emission spectra lines of Eu^{3+} ion are shaped which is due to the screening of 4f orbital by 5s and 5d orbital from crystal field of the host lattice. The spectra have series of peaks well agreeing with the report values of Eu^{3+} emission transition [1, 3, 4]. Figure 9 shows the PL emission spectra of 5 mol% Eu^{3+} doped Y_2O_3 samples prepared by combustion method with different fuels: (1) urea and (2) EDTA-Na_2. It can be seen in the combustion synthesis with EDTA-Na_2 at temperature 350°C that the luminescent intensity of samples increased by near three orders in comparison with that of samples prepared by using urea. This may be due to the formation of well-crystallized cubic yttrium oxide phase [15, 34, 35].

The peaks at 582, 588, 590, 600, 612, and 632 nm are corresponding to the $^5D_0 \rightarrow {}^7F_j$ (j = 0, 1, 2, 3, and 4)

Table 1: Photoluminescence intensity ratios of $^5D_0 \rightarrow {}^7F_2$ to $^5D_0$ of Y_2O_3:5 mol% Eu^{3+} synthesized in using EDTA-Na_2.

Sample name	Sample composition of Eu^{3+} ion	Temperature treatment (°C)	Used fuel	Red/orange $^5D_0 \rightarrow {}^7F_2/{}^5D_0 \rightarrow {}^7F_1$
Y_2O_3:5 mol% Eu^{3+}	5 mol%	350	EDTA-Na_2	10.6
Y_2O_3:5 mol% Eu^{3+}	5 mol%	700	EDTA-Na_2	10.2
Y_2O_3:5 mol% Eu^{3+}	5 mol%	900	EDTA-Na_2	11.3

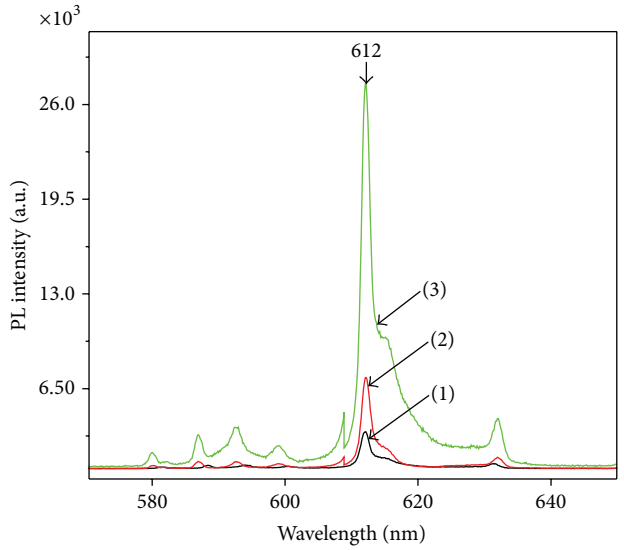

Figure 8: Photoluminescent spectra of Y_2O_3:5 mol% Eu^{+3}. λ_{ex}: curve 1: 254 nm (I : 10), curve 2: 465, and curve 3: 394 nm.

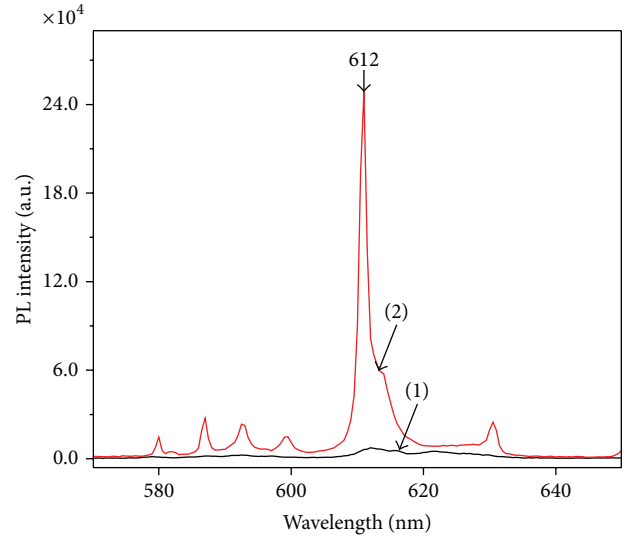

Figure 9: Photoluminescent spectra of Y_2O_3:5 mol% Eu^3. Curve 1: urea; curve 2: EDTA-Na_2.

transition of Eu^{3+} ion in host matrix. The $^5D_0 \rightarrow {}^7F_0$, $^5D_0 \rightarrow {}^7F_2$, and $^5D_0 \rightarrow {}^7F_3$ transitions originate from C_2 sites by electronic dipole transition and the $^5D_0 \rightarrow {}^7F_1$ by magnetic dipole transition situated at both S_6 and C_2 sites [17, 36]. The magnetic dipole transition $^5D_0 \rightarrow {}^7F_1$ is nearly independent of the host matrix and other electric dipoles allowed $^5D_0 \rightarrow {}^7F_j$ (j = 2, 4, and 6) transitions are strongly influenced by the local structure and site asymmetry around the Eu^{3+} ion [4, 25, 37].

Table 1 showed the luminescence intensity ratios of Eu^{3+} ion doped Y_2O_3 matrix. Strong energy transfer from the Eu^{3+} ions occupying S_6 site to C_2 site increased the luminescence efficiency at 612 nm. The photoluminescence intensity ratio of $^5D_0 \rightarrow {}^7F_2$ to $^5D_0 \rightarrow {}^7F_1$ (red to orange) provides valuable information about the site occupied by Eu^{3+} ions and covalent nature of the host matrix. The red/orange ratio of the sample heat treated at different temperatures from 350 up to 900°C only changed very little (10.6–11.3) as shown in Table 1. We suggested that further heat treatment at the higher temperatures will be not necessary.

Figure 10 shows photoluminescent intensity of Y_2O_3:5 mol% Eu^{3+} prepared with EDTA fuel, annealed at 900°C (curve 1), 700°C (curve 2), and 350°C (curve 3). It was indicated that the sample prepared at 350°C exhibited the highest luminescence intensity. The emission intensities from Eu^{3+} rare earth ions were found to increase with the increasing of Eu^{3+} doping from 3 mol% to 5 mol% and to decrease with higher doping content to 7 mol%. It is found that the optimal concentration of Eu^{3+} is 5 mol% and optimal temperature is 350°C.

Figure 11 shows the PL excitation spectra of the Y_2O_3:5 mol% Eu^{3+} nanoparticles. The excitation spectra show a broad peak at 250 nm along with higher side peaks at 395 nm and 465 nm. On increasing the annealing temperature, intensities of higher side peaks are reduced in comparison to 250 nm peak. These characteristic features of Eu^{3+} excitation indicate that at higher annealing temperature the energy required for excitation of nanophosphor is due to the 250 nm peak, which is a charge transfer transition ($Eu^{3+} \leftarrow O^{2-}$) [31].

4. Conclusions

Y_2O_3:Eu^{3+} nanoparticles have been successfully synthesized by the EDTA-Na_2 fuel assisted combustion method at low temperature and in short reaction time. XRD studies confirmed the formation of pure cubic phase of Y_2O_3. The crystalline sizes of the nanoparticles were found to be 24 nm for the samples annealed at ~350°C and 26 nm for the samples annealed at 700°C. The intense peak at 117°C upon UV exposure and at least two peaks at 125 and 336°C upon Gamma irradiation were found in TL process. All the obtained samples showed bright emission under CL or

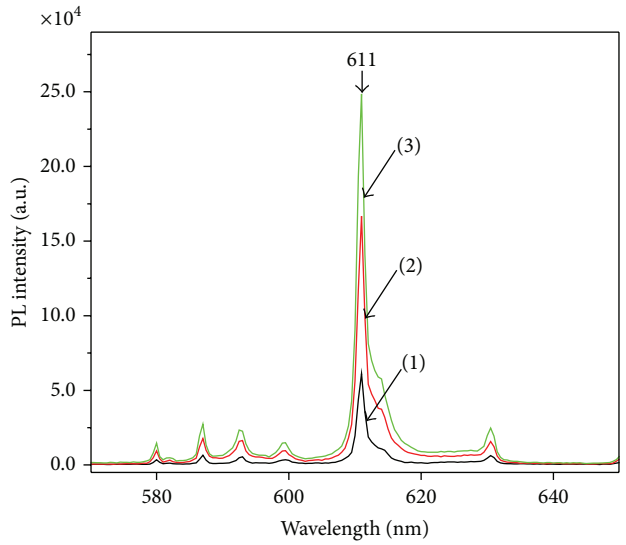

Figure 10: Photoluminescence spectra of Y_2O_3:5 mol% Eu^{3+}. Curve 1: 900, curve 2: 700, and curve 3: 350°C.

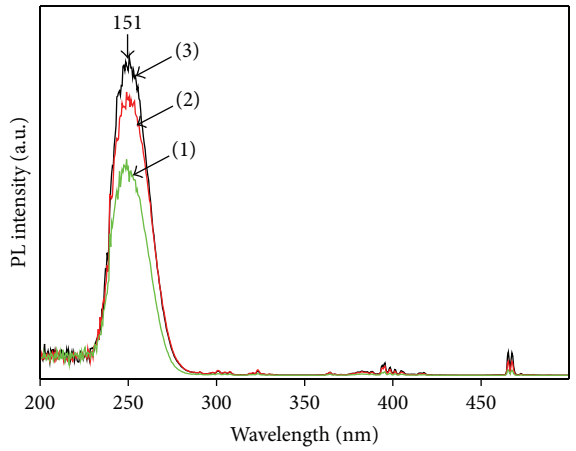

Figure 11: Photoluminescent excitation spectra of Y_2O_3:5 mol% Eu^{3+}. Curve 1: 900, curve 2: 700, and curve 3: 350°C.

PL exciting condition. The PL spectra presented a series of emission peaks between 570 nm and 650 nm corresponding to the $^5D_0$-^7F_j (j = 0, 1, 2, 3, and 4) transition of Eu^{3+} ion. The highest of luminescent intensity at 612 nm under an excitation wavelength of 254 nm is from transition $^5D_0$-$^7F_2$. CL intensity of Y_2O_3:3% mol Eu^{3+} was measured independently on the excitation powers which were 5, 10, and 15 kV. The PL intensity was found to increase with increasing Eu^{3+} doping concentration up to 5 mol%. The nanophosphor Y_2O_3:Eu^{3+} has great potential to develop display and thermoemission dosimeter, especially for biomedical applications.

Conflict of Interests

The authors declare that there is no conflict of interests regarding the publication of this paper.

Acknowledgments

The authors are thankful to the colleagues in the Institute for Research and development High Technology of Duy Tan University; Dr. Vu Thi Thai Ha, Mr. Anh Tuan, and Dr. Nguyen Duc Van in the Institute of Materials Science; and Dr. Do Quang Trung and Ph.D. degree student Nguyen Tu in the Advanced Institute of Science and Technology for CL and PL measurements.

References

[1] L. Q. Minh, W. Strek, T. K. Anh, and K. Yu, "Luminescent nanomaterials," *Journal of Nanomaterials*, vol. 2007, Article ID 48312, 1 page, 2007.

[2] P. Packiyaraj and P. Thangadurai, "Structural and photoluminescence studies of Eu^{3+} doped cubic Y_2O_3 nanophosphors," *Journal of Luminescence*, vol. 145, pp. 997–1003, 2014.

[3] F.-W. Liu, C.-H. Hsu, F.-S. Chen, and C.-H. Lu, "Microwave-assisted solvothermal preparation and photoluminescence properties of Y_2O_3:Eu^{3+} phosphors," *Ceramics International*, vol. 38, no. 2, pp. 1577–1584, 2012.

[4] H. Huang, G. Q. Xu, W. S. Chin, L. M. Gan, and C. H. Chew, "Synthesis and characterization of Eu:Y_2O_3 nanoparticles," *Nanotechnology*, vol. 13, no. 3, pp. 318–323, 2002.

[5] P. Psuja, D. Hreniak, and W. Strek, "Rare-earth doped nanocrystalline phosphors for field emission displays," *Journal of Nanomaterials*, vol. 2007, Article ID 81350, 7 pages, 2007.

[6] J. R. Jayaramaiah, B. N. Lakshminarasappa, and B. M. Nagabhushana, "Luminescence studies of europium doped yttrium oxide nano phosphor," *Sensors and Actuators B: Chemical*, vol. 173, pp. 234–238, 2012.

[7] T. K. Anh, D. X. Loc, T. T. Huong, N. Vu, and L. Q. Minh, "Luminescent nanomaterials containing rare earth ions for security printing," *International Journal of Nanotechnology*, vol. 8, no. 3–5, pp. 335–346, 2011.

[8] A. Gupta, N. Brahme, and D. Prasad Bisen, "Electroluminescence and photoluminescence of rare earth (Eu,Tb) doped Y_2O_3 nanophosphor," *Journal of Luminescence*, vol. 155, pp. 112–118, 2014.

[9] L. Q. Minh, T. Endo, T. T. Huong et al., "Synthesis, structures and properties of emission nanomaterials based on lanthanide oxides and mixoxides," *Transactions of the Materials Research Society of Japan*, vol. 35, no. 6, pp. 417–422, 2010.

[10] J. Zhang, Z. Zhang, Z. Tang, Y. Lin, and Z. Zheng, "Luminescent properties of Y_2O_3:Eu synthesized by sol-gel processing," *Journal of Materials Processing Technology*, vol. 121, no. 2-3, pp. 265–268, 2002.

[11] G. H. Mhlongo, M. S. Dhlamini, H. C. Swart, O. M. Ntwaeaborwa, and K. T. Hillie, "Dependence of photoluminescence (PL) emission intensity on Eu^{3+} and ZnO concentrations in Y_2O_3:Eu^{3+} and ZnO·Y_2O_3:Eu^{3+} nanophosphors," *Optical Materials*, vol. 33, no. 10, pp. 1495–1499, 2011.

[12] C. Feldmann, "Polyol-mediated synthesis of nanoscale functional materials," *Advanced Functional Materials*, vol. 13, no. 2, pp. 101–107, 2003.

[13] Y. Liu, Y. Ruan, L. Song, W. Dong, and C. Li, "Morphology-controlled synthesis of Y_2O_3:Eu^{3+} and the photoluminescence property," *Journal of Alloys and Compounds*, vol. 581, pp. 590–595, 2013.

[14] G. Wakefield, E. Holland, P. J. Dobson, and J. L. Hutchison, "Luminescence properies of nanocrystalline Y_2O_3:Eu^{3+}," *Advanced Materials*, vol. 13, no. 20, pp. 1557–1560, 2001.

[15] G. Siddaramana Gowd, M. Kumar Patra, S. Songara et al., "Effect of doping concentration and annealing temperature on luminescence properties of Y_2O_3:Eu^{3+} nanophosphor prepared by colloidal precipitation method," *Journal of Luminescence*, vol. 132, no. 8, pp. 2023–2029, 2012.

[16] M. Kabir, M. Ghahari, and M. Shafiee Afarani, "Co-precipitation synthesis of nano Y_2O_3:Eu^{3+} with different morphologies and its photoluminescence properties," *Ceramics International*, vol. 40, no. 7, pp. 10877–10885, 2014.

[17] W. Chen, Y. Tong, Y. Liu et al., "Facile synthesis and luminescent properties of Y_2O_3:Eu^{3+} nanophosphors via thermal decomposition of cocrystallized yttrium europium propionates," *Ceramics International*, vol. 39, no. 4, pp. 3741–3745, 2013.

[18] W. Xie, Y. Wang, C. Zou, J. Quan, and L. Shao, "A red-emitting long-afterglow phosphor of Eu^{3+}, Ho^{3+} co-doped Y_2O_3," *Journal of Alloys and Compounds*, vol. 619, pp. 244–247, 2015.

[19] A. M. Khachatourian, F. Golestani-Fard, H. Sarpoolaky, C. Vogt, and M. S. Toprak, "Microwave assisted synthesis of monodispersed Y_2O_3 and Y_2O_3:Eu^{3+} particles," *Ceramics International*, vol. 41, no. 2, pp. 2006–2014, 2015.

[20] Y. Vidya, K. S. Anantharaju, H. Nagabhushana et al., "Combustion synthesized tetragonal ZrO_2: Eu^{3+} nanophosphors: structural and photoluminescence studies," *Spectrochimica Acta Part A: Molecular and Biomolecular Spectroscopy*, vol. 135, pp. 241–251, 2015.

[21] S. T. Mukherjee, V. Sudarsan, P. U. Sastry, A. K. Patra, and A. K. Tyagi, "Annealing effects on the microstructure of combustion synthesized Eu^{3+} and Tb^{3+} doped Y_2O_3 nanoparticles," *Journal of Alloys and Compounds*, vol. 519, pp. 9–14, 2012.

[22] J. A. Capobianco, F. Vetrone, J. C. Boyer, A. Speghini, and M. Bettinelli, "Optical spectroscopy of nanocrystlline, cubic Y_2O_3:Eu^{3+} obtained via combustion synthesis," *Physical Chemistry Chemical Physics*, vol. 2, pp. 3203–3207, 2000.

[23] T. K. Anh, P. Benalloul, C. Barthou, L. T. K. Giang, N. Vu, and L. Q. Minh, "Luminescence, energy transfer, and upconversion mechanisms of y_2O_3 nanomaterials doped with Eu^{3+}, Tb^{3+}, Tm^{3+}, Er^{3+}, and Yb^{3+} ions," *Journal of Nanomaterials*, vol. 2007, Article ID 48247, 10 pages, 2007.

[24] J. Bang, M. Abboudi, B. Abrams, and P. H. Holloway, "Combustion synthesis of Eu-, Tb- and Tm- doped Ln_2O_2S (Ln=Y, La, Gd) phosphors," *Journal of Luminescence*, vol. 106, no. 3-4, pp. 177–185, 2004.

[25] J. R. Jayaramaiah, B. N. Lakshminarasappa, and B. M. Nagabhushana, "Luminescence studies of europium doped yttrium oxide nano phosphor," *Sensors and Actuators, B: Chemical*, vol. 173, pp. 234–238, 2012.

[26] D. Kumar, J. Sankar, K. G. Cho, V. Craciun, and R. K. Singh, "Enhancement of cathodoluminescent and photoluminescent properties of Eu:Y_2O_3 luminescent films by vacuum cooling," *Applied Physics Letters*, vol. 77, no. 16, pp. 2518–2520, 2000.

[27] L. E. Shea, "Low-voltage cathodoluminescent phosphors," *Electrochemical Society Interface*, vol. 7, no. 2, pp. 24–27, 1998.

[28] A. M. Srivastava and C. R. Ronda, "Phosphors," *Electrochemical Society Interface*, vol. 12, no. 2, pp. 48–51, 2003.

[29] X. Liu, C. Lin, and J. Lin, "White light emission from Eu^{3+} in $CaIn_2O_4$ host lattices," *Applied Physics Letters*, vol. 90, no. 8, Article ID 081904, 4 pages, 2007.

[30] N. Brahme, A. Gupta, D. P. Bisen, R. S. Kher, and S. J. Dhoble, "Thermoluminescence and mechanoluminescence of Eu doped Y_2O_3 nanophosphors," *Physics Procedia*, vol. 29, pp. 97–103, 2012.

[31] S.-M. Yeh and C.-S. Su, "UV induced thermoluminescence in rare earth oxide doped phosphors: possible use for UV dosimetry," *Radiation Protection Dosimetry*, vol. 65, no. 1–4, pp. 359–362, 1996.

[32] R. Tamrakar, V. Dubey, N. K. Swamy, R. Tiwari, S. V. N. Pammi, and P. V. Ramakrishna, "Thermoluminescence studies of UV-irradiated Y_2O_3:Eu^{3+} doped phosphor," *Research on Chemical Intermediates*, vol. 39, no. 8, pp. 3919–3923, 2013.

[33] R. K. Tamrakar, D. P. Bisen, I. P. Sahu, and N. Brahme, "UV and gamma ray induced thermoluminescence properties of cubic Gd_2O_3:Er^{3+} phosphor," *Journal of Radiation Research and Applied Sciences*, vol. 7, no. 4, pp. 417–429, 2014.

[34] T. S. Atabaev, H. H. Thi Vu, H.-K. Kim, and Y.-H. Hwang, "The optical properties of Eu^{3+} and Tm^{3+} codoped Y_2O_3 submicron particles," *Journal of Alloys and Compounds*, vol. 525, pp. 8–13, 2012.

[35] T. Igarashi, M. Ihara, T. Kusunoki, K. Ohno, T. Isobe, and M. Senna, "Relationship between optical properties and crystallinity of nanometer Y_2O_3: Eu phosphor," *Applied Physics Letters*, vol. 76, no. 12, pp. 1549–1551, 2000.

[36] M. G. Ivanov, U. Kynast, and M. Leznina, "Eu^{3+} doped Yttrium oxide nanoluminophors from laser synthesis," in *Proceedings of the International Conference on Luminescence and Optical Spectroscopy of Condensed Matter (ICL '14)*, Wroclaw, Poland, July 2014.

[37] G. Y. Hong, B. S. Jeon, Y. k. Yoo, and J. S. Yoo, "Photolumiescence chracteristics of spherica Y_2O_3:Eu^{3+} phosphors by aerosol pyrolysis," *Journal of The Electrochemical Society*, vol. 148, no. 11, pp. H161–H166, 2001.